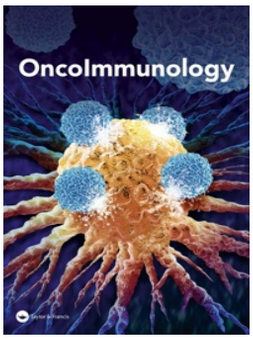

OncoImmunology

ISSN: 2162-402X (Online) Journal homepage: www.tandfonline.com/journals/koni20

Early local immune activation following intra-operative radiotherapy in human breast tissue

Anna Tiefenthaller , Nikko Brix, Roman Hennel , Montserrat Pazos , Bernd Kost , Vera von Bodungen , Brigitte Rack , Rachel Wuerstlein , Benjamin Frey , Udo S. Gaipl , Julia Hess , Kristian Unger , Benedek Dankó , Martin Selmansberger , Horst Zitzelsberger , Nadia Harbeck , Claus Belka , Heike Scheithauer & Kirsten Lauber

To cite this article: Anna Tiefenthaller , Nikko Brix, Roman Hennel , Montserrat Pazos , Bernd Kost , Vera von Bodungen , Brigitte Rack , Rachel Wuerstlein , Benjamin Frey , Udo S. Gaipl , Julia Hess , Kristian Unger , Benedek Dankó , Martin Selmansberger , Horst Zitzelsberger , Nadia Harbeck , Claus Belka , Heike Scheithauer & Kirsten Lauber (2026) Early local immune activation following intra-operative radiotherapy in human breast tissue, OncoImmunology, 15:1, 2653318, DOI: 10.1080/2162402X.2026.2653318

To link to this article: https://doi.org/10.1080/2162402X.2026.2653318

ONCOIMMUNOLOGY
2026, VOL. 15, NO. 1, 2653318
https://doi.org/10.1080/2162402X.2026.2653318

Taylor & Francis
by informa

RESEARCH ARTICLE

OPEN ACCESS Check for updates

Early local immune activation following intra-operative radiotherapy in human breast tissue

Anna Tiefenthaller[a,1], Nikko Brix[a,1], Roman Hennel[a], Montserrat Pazos[a], Bernd Kost[b], Vera von Bodungen[b], Brigitte Rack[b,c], Rachel Wuerstlein[b], Benjamin Frey[d], Udo S. Gaipl[d], Julia Hess[a,e,f], Kristian Unger[a,e,f,g,h], Benedek Dankó[a,e,f,h,i], Martin Selmansberger[e,f], Horst Zitzelsberger[a,e,f], Nadia Harbeck[b], Claus Belka[a,g,h], Heike Scheithauer[a,j] and Kirsten Lauber[a,g,h]

[a]Department of Radiation Oncology, University Hospital, LMU München, Munich, Germany; [b]Breast Center, Department of Obstetrics and Gynecology and CCC Munich, University Hospital, LMU München, Munich, Germany; [c]Department of Gynecology and Obstetrics, Ulm University Hospital, Ulm, Germany; [d]Translational Radiobiology, Department of Radiation Oncology, Universitätsklinikum Erlangen, Friedrich Alexander Universität Erlangen-Nürnberg, Erlangen, Germany; [e]Research Unit Translational Metabolic Oncology, Institute for Diabetes and Cancer, Helmholtz Zentrum München Deutsches Forschungszentrum für Gesundheit und Umwelt (GmbH), Neuherberg, Germany; [f]German Center for Diabetes Research (DZD), Neuherberg, Germany; [g]Bavarian Center for Cancer Research (BZKF) Partner Site Munich, Germany; [h]German Cancer Consortium (DKTK) Partner Site, Munich, Germany; [i]German Cancer Research Center (DKFZ), Heidelberg, Germany; [j]Nordstrahl Radiation Oncology Unit, Nürnberg North Hospital, Nürnberg, Germany

ABSTRACT

The local immune effects of cancer radiotherapy remain poorly characterized in humans due to limited access to irradiated tissue. Mechanistic insights largely derive from preclinical models employing tumor-intact, neoadjuvant-like settings. Here, we present real-world immunoprofiling data from breast cancer patients undergoing breast-conserving surgery with ($n = 20$) or without ($n = 29$) intraoperative radiotherapy (IORT). Postoperative wound fluid samples were analyzed by flow cytometry, multiplex cytokine profiling, and bulk RNA-sequencing, alongside systemic immune monitoring in peripheral blood. IORT triggered rapid local accumulation of distinct innate immune cell subsets and cytokines mediating recruitment, activation, and innate-adaptive crosstalk, accompanied by systemic features consistent with emergency hematopoiesis. Transcriptomic profiling of wound fluid mononuclear cells revealed enrichment of proinflammatory IL-6-JAK/STAT3 signaling. *In vitro,* irradiation of primary breast tissue cells recapitulated key cytokine patterns and led to robust senescence induction, suggesting irradiated, senescent normal tissue cells as drivers of early immune activation in postsurgical radiotherapy. These data provide direct clinical evidence that radiotherapy shapes local and systemic immune responses, offering mechanistic insights with clear relevance for tumor immunology and the development of rational radiotherapy–immunotherapy combination strategies.

ARTICLE HISTORY

Received 19 November 2025
Revised 5 March 2026
Accepted 26 March 2026

KEYWORDS

Breast cancer; immune cell recruitment; innate immune cells; eosinophils; monocytes; plasmacytoid dendritic cells; MIF; IL-3; Intra-operative radiotherapy (IORT)

CONTACT Kirsten Lauber Kirsten.lauber@med.uni-muenchen.de Department of Radiation Oncology, University Hospital, LMU München, Marchioninistr. 15, 81377, Munich, Germany
[1] These authors contributed equally to this work.
Supplemental data for this article can be accessed online at https://doi.org/10.1080/2162402X.2026.2653318.

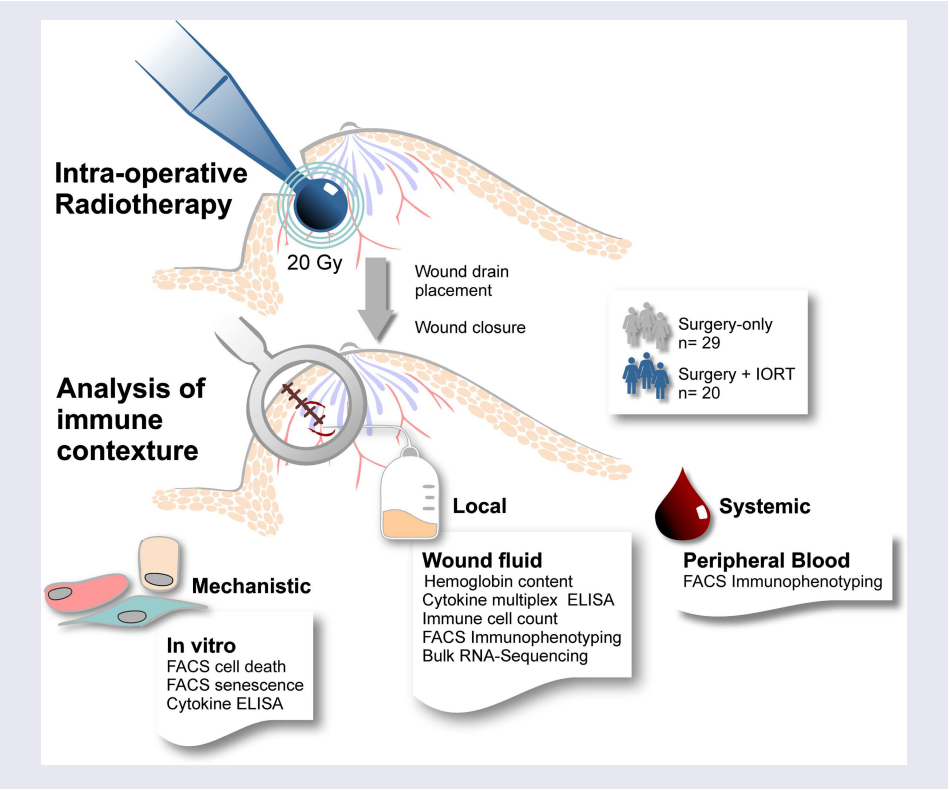

Introduction

The immune-modulating properties of cancer radiotherapy have been intensively studied in recent years and are meanwhile framed conceptually as *in situ* vaccination phenomena capable of (re-)activating antitumor immunity, particularly when combined with immunotherapy.[1-4] Importantly, however, mechanistic insights into local immune (re-)activation by radiotherapy predominantly stem from preclinical models, where tumors are typically present. Often transplanted heterotopically, i.e. distant from the corresponding normal parenchymal tissue, these tumors are irradiated in a neoadjuvant-like setting. In this scenario, radiation-induced immunogenic forms of tumor cell death and the corresponding release of damage-associated molecular patterns (DAMPs) have been delineated as major determinants of innate immune cell recruitment and activation.[5-7] While informative, such experimental conditions tend to overrepresent tumor cell-driven immune effects, leaving the contribution of the irradiated normal tissue unclear.

In the clinical routine, however, radiotherapy is most often administered in postoperative, adjuvant situations, where little or no tumor burden remains within the radiation field. Here, the primary target of irradiation is the normal tissue in the former tumor bed, which may harbor only interspersed subclinical residual tumor cells. To date, it remains elusive how the local immune contexture is altered in this setting, both in terms of upstream drivers and downstream effector mechanisms. The lack of access to serial, site-specific human tissue samples in postsurgical irradiation scenarios has consistently impeded the direct assessment of early immune-related changes in irradiated normal tissue.

This is where intraoperative radiotherapy (IORT) offers a unique opportunity. In IORT, irradiation is delivered immediately after surgical removal of the tumor. A single high dose of low-energy photon or electron radiation is applied directly to the exposed tumor bed. The steep dose gradient limits radiation exposure to normal tissue located within a very narrow margin around the radiation applicator, without encompassing the draining lymph nodes (**Figures S1A** and **S1B**).[8-10] Prior to wound closure, a drainage system is connected to the irradiated site, allowing continuous collection of accumulating wound fluid. This wound fluid can serve as a surrogate biospecimen for interrogating the local immune environment

within the irradiated tumor bed, enabling direct, site-specific investigation of early immune responses in humans in a clinically relevant context.

We took advantage of this clinical scenario and conducted an observational study in breast cancer patients undergoing breast-conserving surgery with IORT ($n = 20$) or without IORT ($n = 29$) (single dose of 20 Gy low-energy photons). This approach enabled us to examine immediate, local immune responses to radiation within the former tumor bed. Wound fluid was collected via surgical drains from post-operative days 1 to 3, allowing for comprehensive analysis of local immune responses. We assessed fluid volume, cellularity, and hemoglobin content, and performed flow cytometry-based immunomonitoring, multiplex cytokine profiling, and bulk RNA-sequencing of wound fluid mononuclear cells. In addition, peripheral blood samples were obtained preoperatively (day −1), early postoperatively (day 3), and at follow-up (day 28) to capture systemic immune dynamics. This study design provided a valuable opportunity to dissect early, radiation-induced immune perturbations in humans under real-world conditions. In parallel, we recapitulated the IORT setting by irradiating primary breast epithelial cells, normal fibroblasts, and endothelial cells *in vitro*, followed by analyses of cell fate decisions and cytokine release.

We observed marked alterations of the immune contexture in the tumor bed upon IORT, with significant accumulation of distinct innate immune cell populations, including plasmacytoid dendritic cells (pDCs), eosinophils, and monocytes compared to surgery-only controls. Innate immune cell counts correlated with elevated MIF and IL-3 levels in the wound fluid—cytokines implicated in monocyte and eosinophil trafficking and emergency hematopoiesis. Bulk RNA-sequencing of wound fluid mononuclear cells confirmed upregulation of inflammatory cytokine signaling pathways. Importantly, the postsurgical clinical situation and our data suggest that these immune alterations are predominantly driven by irradiated normal tissue cells within the tumor bed, rather than residual tumor cells. Complementary *in vitro* modeling of IORT conditions further revealed a strong induction of normal tissue cell senescence and the release of senescence-associated cytokines upon radiation, highlighting a potential mechanism of local immune activation in postsurgical radiotherapy settings.

Materials and methods

Study design and patient inclusion

The study involved female breast cancer patients undergoing breast-conserving surgery ± intraoperative radiotherapy (IORT) at LMU University Hospital (Department of Obstetrics and Gynecology and Department of Radiation Oncology). IORT was administered based on routine clinical criteria rather than within a clinical trial. The study was conducted between 2015 and 2025 (patient recruitment 2015–2018, biosample analyses 2015–2025) in accordance with the Declaration of Helsinki and was approved by the Ethics Committee of the LMU Munich Medical Faculty (approval numbers 246-15 and 20-488). Written informed consent was obtained from all participants prior to inclusion. Eligible patients had histologically confirmed breast cancer scheduled for breast-conserving surgery with or without intraoperative radiotherapy (IORT). To minimize immunological confounders, patients receiving immunomodulatory drugs or presenting with immune-related diseases were excluded. Patients who had received neoadjuvant chemotherapy within eight weeks before surgery were also excluded. Data analysis was performed using anonymized data.

Wound fluid and blood sampling

All experiments involving human-derived materials (wound fluid, peripheral blood) were conducted in compliance with institutional biosafety regulations under biosafety level 2 (BSL-2) conditions, including the use of appropriate personal protective equipment and waste disposal procedures. Peripheral blood samples were collected preoperatively (day −1), postoperatively during hospitalization (day 3), and during patient follow-up (day 28). Blood was collected in EDTA tubes (Sarstedt, Cat#01.1605.001). Wound fluids were collected from breast surgical drains on postoperative day 1 to day 3 for cellular and humoral

analyses. Axillary drain fluids were excluded from analysis. Upon collection, wound fluid volume was measured, and samples were processed for humoral, cellular, and molecular analyses.

Quantification of key wound fluid parameters

Wound fluid and EDTA whole blood were assessed for volume, hemoglobin content and leukocyte count. Erythrocyte lysis was performed on 100 µL of EDTA blood or wound fluid using 1 mL (blood) or 3 mL (wound fluid) of 1 × Pharm Lyse lysing buffer (BD Biosciences, Cat#555899), incubated for 20 min at room temperature with intermittent inversion. Samples were centrifuged (5 min, 314 × g), washed with DPBS, and leukocytes were resuspended in the initial sample volume. Leukocyte counts were determined both manually via Neubauer chamber and by flow cytometry using counting beads. For flow cytometry, 100 µL of lysed sample was stained with 6 µL anti-CD45-BUV395 (BD Biosciences, Cat#563791), incubated in the dark (20 min), washed, resuspended in FACS staining buffer (BD Biosciences, Cat#554656), and supplemented with 10 µL Count Bright absolute counting beads (Invitrogen, Cat#36950) prior to acquisition with an LSR II cytometer (BD Biosciences). Manual and flow cytometric counts were averaged for downstream analyses. For hemoglobin analysis, 5 µL of EDTA whole blood or wound fluid was diluted in 0.9% NaCl (w/v) (1×, 1 + 1, 1 + 4, 1 + 9) and added to 250 µL Drabkin's solution (1 vial Drabkin's reagent (Sigma-Aldrich, Cat#D5941) + 1 ml ddH_2O + 0.5 ml 30% Brij-L23 solution (Sigma-Aldrich, Cat#B4184)). A standard curve was prepared from serial dilutions of human hemoglobin EightCheck-3WP-*N* (Sysmex, Cat#90406116). Absorbance was measured in technical triplicates at 540 nm with background correction at 680 nm using a SynergyMx plate reader (BioTek Instruments).

Analysis of immune cell subpopulations

Leukocyte subpopulations in blood and wound fluid were analyzed by flow cytometry (antibodies listed in **Table S1**). For each analysis, 100 µL of EDTA-anticoagulated whole blood or wound fluid was used. Blood samples were stained with the antibody panel or matched isotype controls for 20 minutes at 4°C in the dark, followed by erythrocyte lysis using 1 × Pharm Lyse (BD Biosciences, Cat#555899) as described above. Wound fluid samples were subjected to an initial erythrocyte lysis step prior to antibody staining, followed by a second lysis after staining to remove residual erythrocytes. After lysis and washing, cells were stained with the antibody panel or matched isotype controls (20 minutes, 4°C). Cells were then washed twice with FACS buffer (BD Biosciences, Cat#554656), resuspended in the original sample volume, and acquired on an LSR II flow cytometer (BD Biosciences). After debris and doublet exclusion, leukocyte subsets were defined through sequential gating using FACSDiva software (BD Biosciences) as illustrated in **Figure S2A**. Frequencies were calculated as percentages of $CD45^+$ cells. For wound fluid, absolute counts of each leukocyte subset were additionally determined.

Wound fluid processing of cytokines and mononuclear cells

Residual wound fluid was preserved for downstream analyses. For mononuclear cell preparation, wound fluid was centrifuged (10 min, 200 × g, brake off), supernatants discarded, and the leukocyte buffy coat collected. Leukocytes were purified by Biocoll gradient centrifugation (Biochrom AG, Cat#L6115; 20 min at room temperature, 787 × g, brake off), washed in DPBS, and resuspended in cold freezing medium consisting of 90% (v/v) FCS and 10% (v/v) DMSO (Sigma-Aldrich, Cat#D2650). Cells were cryopreserved and stored in liquid nitrogen. Separately, wound fluid supernatants intended for multiplex ELISAs were generated by centrifugation (1,200 × g, 3 min, 4°C), followed by a clearing spin at 14,000 × g for 3 min (4°C). Supernatants were shock-frozen in liquid nitrogen and stored at −80°C.

Multiplex ELISA of wound fluid cytokines

Cytokine and chemokine profiling was performed with wound fluids from postoperative day 2 using Bio-Plex Pro Human Chemokine assays (40-plex and 48-plex panels; Bio-Rad, Cat#171AK99MR2 and

Cat#12007283, respectively). Samples were thawed on ice, diluted 1 + 4 in assay buffer and further steps were performed according to the manufacturer's instructions. Readout was conducted using a Bio-Plex 200 system (Bio-Rad).

Singleplex ELISAs for selected cytokines from wound fluid and primary cell culture supernatants

Cytokines not covered by the multiplex panels (40-plex and 48-plex), specifically XCL1 and Flt3-Ligand, were measured by singleplex ELISA (R&D Systems, Cat#DY695 and Cat#DY308, respectively) in day 2 wound fluids. Similarly, MIF, IL-3, and HGF were quantified in primary cell culture supernatants from HMECs, HUVECs, and NHDF-Ad irradiated with 0–20 Gy using singleplex ELISAs. To obtain supernatants from *in vitro* cultures, commercially available primary human cells were purchased. Cells were grown in humidified incubators (37°C, 5% CO_2) in supplemented growth media (see **Table S1** for details) and seeded into 24-well plates (45,000–60,000 cells/well) in 400 µL of appropriate culture medium. Cells were allowed to adhere for 16–24 h before the medium was replaced (400 µL/well), and cells were subsequently irradiated with 0–20 Gy using an RS-225 x-ray cabinet (Xstrahl) operated at 200 kV and 10 mA (Thoraeus filter, 1 Gy in 242 s). After 48 hours, cell-free supernatants were collected on ice, centrifuged at 13,000 × g for 1 min at 4°C, and aliquoted into prechilled tubes. Samples were snap-frozen in liquid nitrogen and stored at −80°C until analysis. All assays were performed using DuoSet® ELISA kits (R&D Systems, Cat#DY289, Cat#DY203 and Cat#DY294, respectively) according to the manufacturer's instructions. Wound fluid was analyzed at 1 + 4 dilution, primary cell supernatants were used undiluted or 1 + 1 diluted depending on the analyte. Absorbance was measured at 450 nm using a SynergyMx microplate reader, and concentrations were calculated from standard curves.

Cell death analysis by Annexin V/PI staining

Apoptotic and necrotic cell death of HMECs, NHDF-Ad, and HUVECs postirradiation (days 1–4) was assessed by flow cytometry using Annexin V-FITC and propidium iodide (PI) staining. Cells were detached with TrypLE Express (Gibco, Cat#12604-039), washed, and stained for 15 min on ice in the dark using a staining mix containing 5 µl Annexin V-FITC (BD Biosciences, Cat#556419), 0.2 µl PI (Sigma-Aldrich, Cat#P4170), and 94.8 µl 1 × Annexin V binding buffer (BD Biosciences, Cat#556454). After washing, cells were resuspended in staining buffer and analyzed by flow cytometry. Annexin V-positive/PI-negative cells were classified as apoptotic, double-positive as necrotic, and double-negative as viable.

Senescence detection via flow cytometry

Primary cells were cultured in sixwell plates (5000–50000 cells/well) and cellular senescence was quantified by flow cytometry using the fluorogenic substrate C_{12}-FDG (5-Dodecanoylaminofluorescein di-β-D-Galactopyranoside, Marker Gene Technologies, Cat#MGT-M2888-M005) to detect senescence-associated β-galactosidase (SA-βgal) activity.[11] Lysosomes were alkalinized by incubating cells for 1 h (37°C, 5% CO_2) in serum-free medium with 100 nM Bafilomycin A1 (LC Laboratories, Cat#B-1080), prior to addition of 50 µM C_{12}-FDG (1 h, 37°C, 5% CO_2). Cells were then harvested, resuspended in cooled DPBS, and analyzed by flow cytometry. Cells exhibiting high SA-βgal signal together with increased sideward scatter (SSC) were classified as senescent.

Bulk 3'-RNA-sequencing of mononuclear cells

Cryopreserved immune cells from day 2 wound fluids enriched by density gradient centrifugation as described above were rapidly thawed and resuspended in cold DPBS. After centrifugation (314 g, 4°C, 5 min) and washing, total RNA was extracted using the NucleoSpin® miRNA Kit (Macherey & Nagel, Cat#740971.250) and eluted in 50 µL nuclease-free water. RNA concentration was measured with a NanoDrop 2000c spectrophotometer (Thermo Fisher Scientific). Libraries were

prepared using the QuantSeq 3′mRNA-Seq Library Prep Kit for Illumina (FWD, Lexogen, Cat#015.24), and sequencing was performed as previously described.[12] Differential gene expression analysis between IORT and controls was carried out with the R library DESeq2.[13] Preranked gene set enrichment analysis was performed using the R library fGSEA[14] with gene ranks as −log10(*p*-value) × log2(fold difference) using the immune-related subset of the Hallmark gene sets collection from the Molecular Signatures Database (MsigDB).[15] Expression data was variance stabilizing transformed (VST) or z-scored for visualization purposes with the R library DESeq2. The Cytoscape app 3.10.1 version was utilized for creating the Reactome FI network with the selected pathway leading edge genes.[16,17]

Statistical analysis

Statistical analyses were performed in OriginPro2024, unless stated otherwise. Immune cell subset comparisons in wound fluids used exact Wilcoxon rank tests with Benjamini–Hochberg correction. Serial peripheral blood-derived data were analyzed using one-way ANOVA of repeated measures (factor: postoperative day). Cytokine amounts in wound fluids were compared using exact Wilcoxon rank tests. To assign patterns of similarity, unsupervised hierarchical clusterings of sample-to-sample, cell type-to-cell type, or cytokine-to-cytokine correlations (Spearman's ρ) were generated (1 − Pearson correlation as distance metrics). Expression patterns of leading-edge genes (RNA z-scores) were clustered similarly (Euclidean distance as metric).

Results

IORT induces local accumulation of distinct innate immune cell subsets in the irradiated tumor bed

In this prospective observational study, we analyzed postsurgical wound fluid samples from breast cancer patients to characterize cellular and humoral changes in the local immune microenvironment following IORT (Figure 1A). The study population included an IORT group ($n = 20$) and a surgery-only control group ($n = 29$), with baseline clinical characteristics broadly comparable between groups (**Figures S1C–S1F** and **Table S2**). In line with current clinical practice, where IORT is typically offered to selected older patients with early-stage breast cancer to reduce or replace the need for postoperative external beam radiotherapy, the IORT group in our study was slightly older and had tumors with a tendency towards lower stage and grade. Molecular tumor features, including Ki-67 proliferation index, receptor status, and intrinsic subtype did not differ significantly.

Wound fluid was collected from surgical drains on three consecutive days, and no significant differences in volume or hemoglobin content were found between groups (Figure 1B and C). Elevated hemoglobin levels on day 1 suggested a predominant contribution of postsurgical bleeding rather than lymphatic immune cell recruitment or retention. This is in line with previous reports, in which analyses of day 1 wound fluid samples yielded inconclusive results, likely early blood contamination masking immune-related signals.[18] The blood contamination was markedly reduced on postoperative days 2 and 3, making these time points the focus of our analysis. Day 2 samples consistently provided sufficient wound fluid volume to perform all planned analyses. In contrast, day 3 wound fluid volumes were very limited in a substantial proportion of patients (13 cases across both treatment groups with ≤5 ml, Figure 1). While this allowed basic biophysical assessments (volume, hemoglobin content, leukocyte count), it was insufficient for more input-intensive analyses such as multicolor FACS, multiplex cytokine measurements, and preparation of wound fluid mononuclear cells for bulk RNA-sequencing. Consequently, detailed immune profiling was focused on day 2. Total leukocyte counts trended higher in IORT samples on postoperative days 2 and 3 but did not reach statistical significance (Figure 1D).

We analyzed wound fluids of day 2 after surgery ± IORT via multicolor flow cytometry and determined total cell counts of different immune cell populations (gating strategy in **Figure S2A**). Three innate immune cell subsets—plasmacytoid dendritic cells (pDCs), eosinophils, and monocytes—were significantly enriched in the wound fluids of IORT-treated patients compared

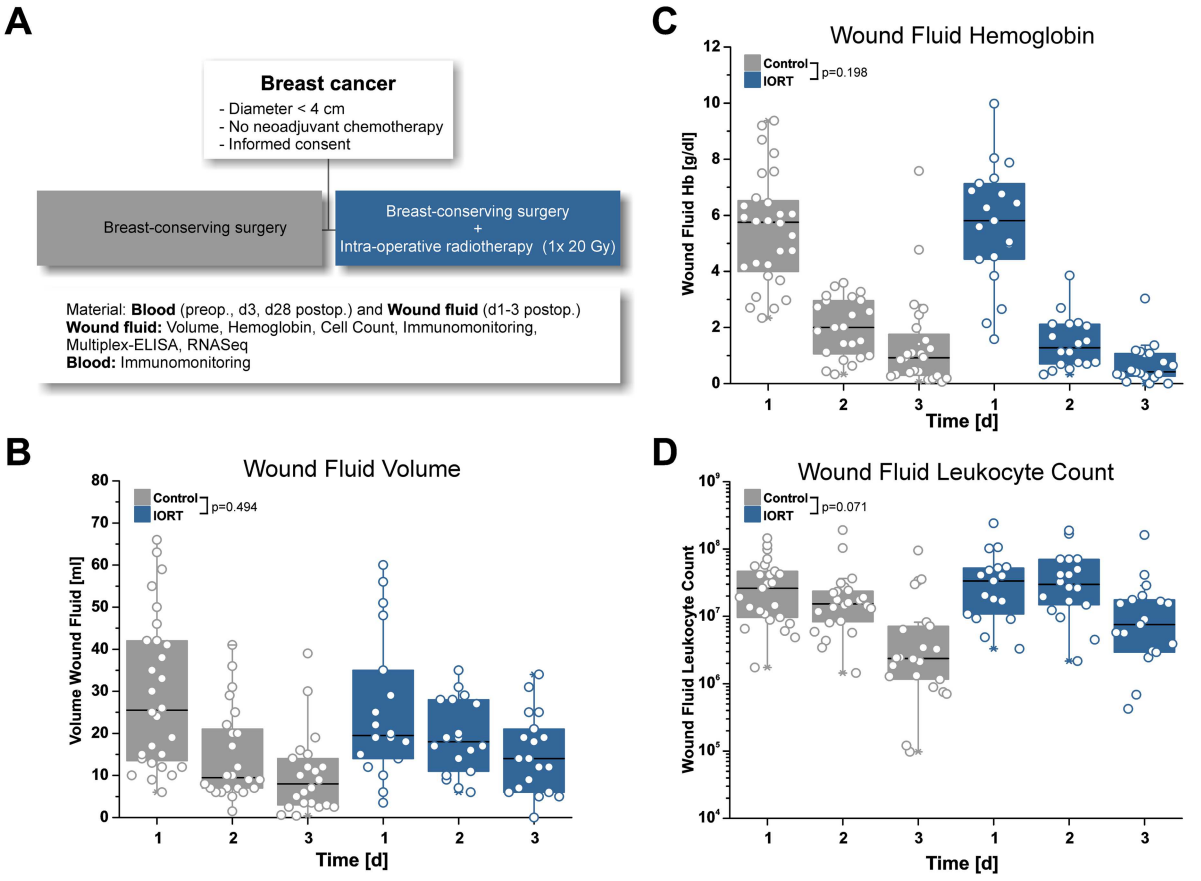

Figure 1. Study design and biophysical characteristics of postsurgical wound fluids in breast cancer patients. (A) Overview on study design and patient recruitment of IORT and control group with inclusion criteria (top), biosamples, and analyses. See also **Figure S1** and **Table S2**. (B–D) Overview on the total volume of wound fluid, the hemoglobin content as a measure of passive bleeding, and the total leukocyte counts on days 1–3 after surgery ± IORT. Each data point represents one sample of one individual patient. Statistical analysis was performed using two-way ANOVA; shown are *p*-values for the factor "treatment group".

to surgery-only controls (Figure 2, **Table S3**). Among monocyte subsets, $CD14^{+}CD16^{-}$ classical monocytes showed the most pronounced enrichment compared to intermediate ($CD14^{+}CD16^{+}$) and nonclassical ($CD14^{dim}CD16^{+}$) subsets (Figure 2A-E), indicating preferential recruitment/retention of classical monocytes as key early responders in tissue inflammation following IORT. Unsupervised hierarchical clustering revealed a strong positive correlation in total cell counts between monocytes and eosinophils, suggesting that these cell types may follow coordinated recruitment/retention in (to) the tumor bed after IORT rather than accumulating independently (Figure 2B). B cell counts were also elevated in IORT wound fluid samples, but displayed a distinct pattern with less similarity to other immune cell subsets (Figure 2A and B). pDCs exhibited the strongest accumulation upon IORT while showing minimal correlation with other enriched populations, consistent with unique mechanisms of recruitment/retention (Figure 2A, B, and E). In contrast, the abundance of other immune cell types, including basophils, classical dendritic cells (cDCs), and all other lymphocyte subsets analyzed, remained largely unaffected, highlighting the selective nature of the local immune alterations in the early time window after irradiation analyzed (Figure 2A). This pattern, dominated by distinct innate immune cell infiltration on day 2 after radiation treatment, is highly reminiscent of recruitment dynamics known from other scenarios of sterile inflammation.[19] Exploratory analyses of the remaining day 3 samples (16 IORT vs. 20 surgery-only cases) showed similar trends for pDCs, eosinophils, and monocytes, consistent with the selective innate recruitment observed on day 2. However, statistical significance was not reached due to the limited sample size (data not shown).

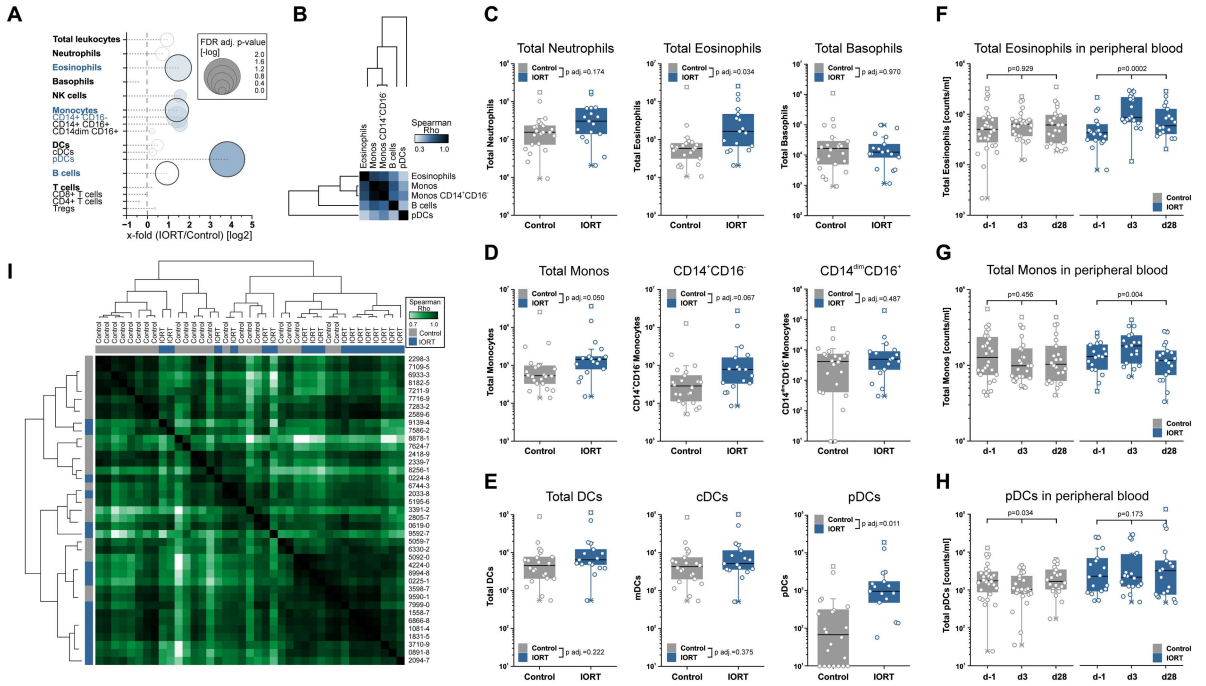

Figure 2. IORT triggers local accumulation and systemic mobilization of distinct innate immune cell subsets. (A) Relative abundance of immune cell subsets in IORT ($n = 17$) versus control ($n = 22$) wound fluid samples on day 2 post surgery. Color intensity reflects fold difference of median values ($\log_2$ scale). Circle size reflects statistical significance of subset-wise comparisons as $-\log_{10}$ of FDR-adjusted p-values from exact Wilcoxon rank tests, corrected using the Benjamini–Hochberg procedure (see also **Table S3**). Immune cell populations with FDR-adjusted p-values < 0.1 are highlighted in blue. (B) Correlation matrix of absolute cell counts for immune cell subsets elevated in IORT day 2 wound fluid samples. Spearman's ρ and unsupervised hierarchical clustering are shown (1 − Pearson correlation as distance metric). (C–E) Flow cytometric quantification of different immune cell (sub-)populations in day 2 wound fluid samples. (F–H) Time course analyses of total immune cell counts per ml in peripheral blood measured by flow cytometry. Each dot in subfigures C–H represents one individual patient sample. Statistical analyses were performed using the exact Wilcoxon rank test with Benjamini–Hochberg correction for comparison of wound fluid samples (C–E) and one-way ANOVA of repeated measures (factor: postoperative day) for serial blood samples (F–H). (I) Sample-to-sample correlation of absolute immune cell counts in day 2 wound fluid samples. Unsupervised hierarchical clustering of Spearman's correlation coefficients ρ (1 − Pearson correlation as the distance metrics). For flow cytometry gating strategy, see also **Figure S2**.

Distinct innate immune cell populations enriched in IORT wound fluids exhibit transient systemic mobilization

Based on the local effects observed in wound fluids, we next examined whether IORT also induced systemic changes by analyzing serial peripheral blood samples. Following surgery, total leukocyte counts in peripheral blood declined transiently (**Figure S2B-C**). This was primarily driven by a significant decrease in circulating neutrophils and is a well-known phenomenon attributed to peripheral tissue trapping and margination of neutrophils.[20] Notably, however, IORT attenuated and—in part—inverted this dynamic profile for specific immune cell subsets (Figure 2F-H and **Figures S2B** and **S2C**). Total monocytes, classical monocytes, and eosinophils exhibited a significant transient increase in circulation following IORT, peaking on day 3 and declining by day 28 after surgery (Figure 2F and G), while systemic pDC levels remained virtually unchanged following IORT (Figure 2H). These findings suggest that IORT can elicit a transient systemic mobilization of selected innate immune cell subpopulations, likely driven by early local signals and resembling emergency hematopoiesis known from other settings of sterile inflammation.[21] Consistent with distinct subsets of innate immune cell populations being differentially enriched in IORT wound fluids, sample-to-sample correlation based on innate immune cell composition did not yield a complete, but a reasonable separation of IORT and control samples by treatment group. Cluster 1 comprised 13/16 (81%) control samples, whereas 14 of 25 (56%) samples in Cluster 2 were from IORT-treated patients, indicating an obvious radiation-induced shift in local immune infiltration profiles (Figure 2I).

Cytokine profiling of IORT wound fluids identifies innate recruitment factors secreted by irradiated non-malignant cells in vitro

To identify candidate mediators of innate immune cell recruitment and/or retention following IORT, we performed unbiased multiplex profiling of 69 cytokines in day 2 wound fluid samples and correlated total cytokine amounts with immune cell counts (Figure 3A, **Table S4**). Among the top five cytokines showing strong positive correlations (Spearman's $\rho > 0.5$) were macrophage migration inhibitory factor (MIF) and

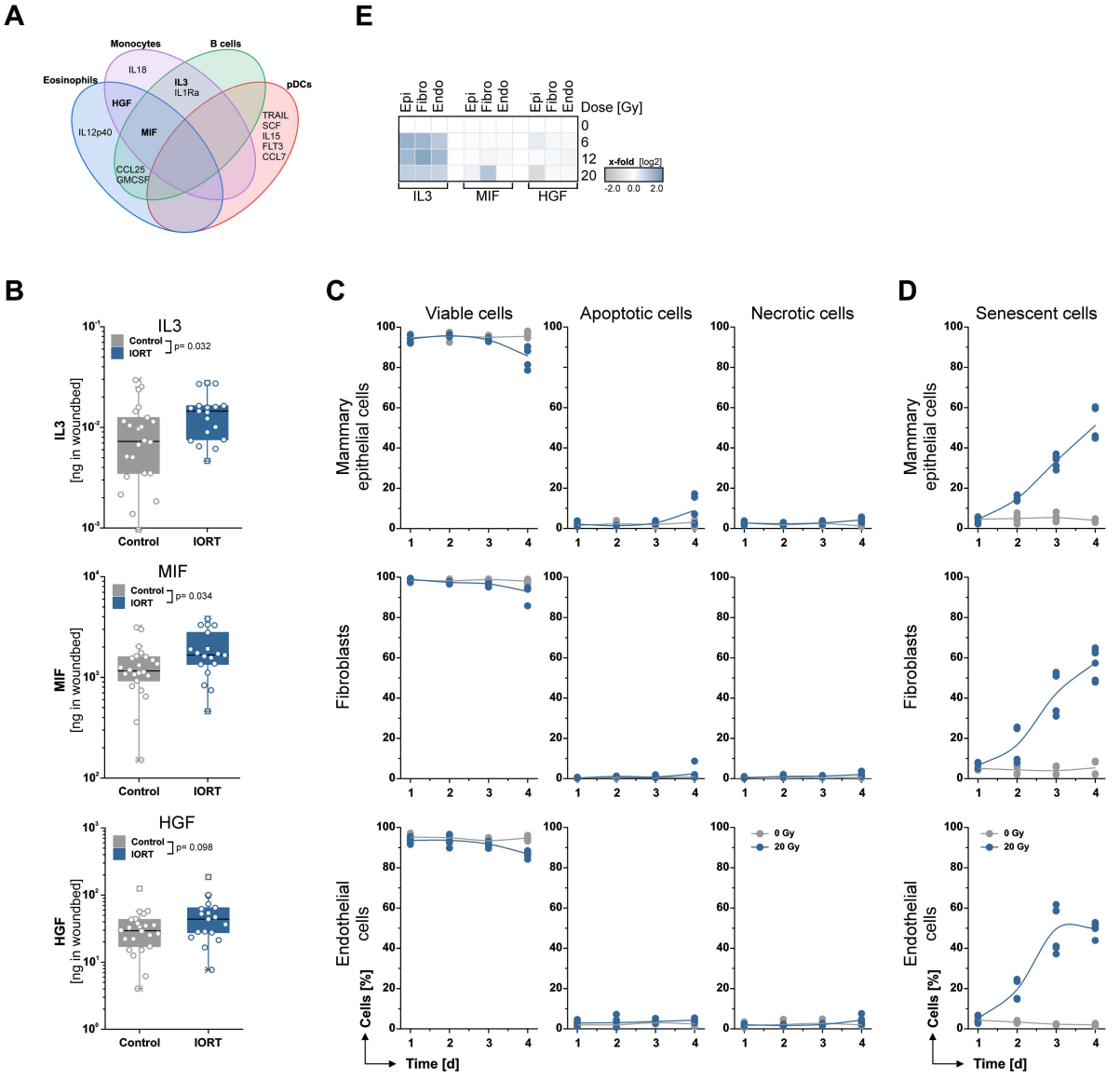

Figure 3. Cytokine profiling of IORT wound fluids identifies innate recruitment factors secreted by irradiated non-malignant cells *in vitro*. (A) Venn diagram showing the top five cytokines correlating with immune cell subset counts significantly elevated upon IORT. Absolute cytokine levels in day 2 wound fluid (IORT ($n = 17$) vs control ($n = 22$)) were measured by multiplex ELISA and correlated with total immune cell counts (see also Figure 2). Key cytokines highlighted in bold indicate Spearman's $\rho > 0.5$ and rank among the top five correlating cytokines for more than one cell subset. See also **Figure S3** and **Table S4**. (B) Absolute amounts of key cytokines identified in (A) in day 2 wound fluid samples. Statistical differences between IORT and control group were determined by exact Wilcoxon rank test. (C–D) Flow cytometric analysis of cell fates in primary human mammary epithelial cells, fibroblasts, and endothelial cells. Viability, apoptosis, and necrosis were assessed by annexin V/propidium iodide staining shown in (C), and senescence was evaluated by quantifying SSC^{hi} cells with elevated β-galactosidase activity in C_{12}-FDG staining (D). Technical triplicates from two independent biological replicates are shown. (E) Release of IL-3, MIF, and HGF from primary mammary epithelial cells (HMECs), fibroblasts, and endothelial cells on day 2 after irradiation *in vitro*. Cytokine concentrations were determined by ELISA in technical triplicates of which the means, normalized to the 0 Gy controls, are displayed.

hepatocyte growth factor (HGF), both closely associated with eosinophil and monocyte counts, as well as interleukin-3 (IL-3), which correlated with total and classical monocyte counts. In line with their distinct accumulation pattern, pDCs displayed the strongest correlations with a separate set of cytokines. However, the substantial proportion of control samples lacking detectable numbers of pDCs impaired the robustness of these correlation analyses. Notably, the wound fluid amounts of MIF and IL-3 were significantly elevated in IORT samples compared to controls, supporting their possible involvement in local recruitment processes, whereas the difference in HGF did not reach statistical significance (Figure 3B).

Given the postsurgical nature of the IORT setting, these cytokine alterations are unlikely to be tumor cell-driven. Instead, irradiated nonmalignant cells within the former tumor bed are the most plausible source. Due to the steep dose gradient of IORT, radiation exposure is confined primarily to breast epithelial cells, fibroblasts, and—to a lesser extent—endothelial cells in close proximity to the applicator (**Figures S1A** and **S1B**). To test this, we recapitulated the clinical scenario *in vitro* by irradiating primary human breast epithelial cells, fibroblasts, and endothelial cells and assessed their cytokine secretion profiles and cell fate responses. Viability of all three cell types remained largely preserved over four days postirradiation, with only minimal apoptotic or necrotic cell death observed (Figure 3C). Instead, a robust senescence response was induced, as evidenced by increasing senescence-associated β-galactosidase activity from day 2 onwards, with approximately 50% of cells exhibiting a senescent phenotype by day 4 (Figure 3D). These findings confirm cellular senescence as the predominant response of nonmalignant breast tissue cells to high-dose irradiation. We measured the release of MIF, IL-3, and HGF by primary human mammary epithelial cells, fibroblasts, and endothelial cells following irradiation, acknowledging that IL-3 production by these cell types is generally not anticipated. Since IORT delivers 20 Gy only at the applicator surface, with a steep dose fall-off in adjacent breast tissue (**Figures S1A** and **S1B**),[8] we assessed cytokine secretion across the dose range of 0–20 Gy to capture the gradient of radiation exposure encountered by nonmalignant cells *in situ*. Elevated MIF release was observed in mammary epithelial cells and fibroblasts, but only at the highest dose of 20 Gy, whereas endothelial cells showed no radiation-induced MIF secretion (Figure 3E). In contrast, IL-3 release increased already at lower irradiation doses in all three cell types tested, and HGF secretion remained unaffected by radiation. These results indicate that different nonmalignant breast tissue cells can produce MIF and IL-3 in a radiation dose-dependent manner, supporting their contribution to the local cytokine milieu associated with innate immune cell recruitment following IORT.

Importantly, MIF and IL-3 are not solely involved in immune cell recruitment, but also contribute to emergency hematopoiesis and myelopoiesis, activation of innate immune cells, and the coordination of adaptive cytotoxic responses.[22-4] Consistent with this, IORT wound fluids exhibited elevated amounts of additional cytokines known to support immune cell activation, differentiation, and innate-adaptive cross-talk, including macrophage colony-stimulating factor (M-CSF), interleukin-12p40 (IL-12p40), interferon alpha 2 (IFN-α2), interleukin-15 (IL-15), and interferon gamma (IFN-γ) (**Figure S3A**). Cytokine-to-cytokine correlation analyses revealed clusters of cytokines with shared abundance patterns in wound fluid samples indicative of common upstream regulation, as supported by functional interaction networks (**Figure S3B**). Among these, we identified three clusters associated with NFKB1/FOS, RELA/RELB-, and REL/RELA/CEBPB/STAT3 signaling. Intriguingly, all cytokines elevated in IORT wound fluids were part of the latter, implicating CEBPB and STAT3 as key early transcriptional regulators of the radiation response in nonmalignant breast tissue.

Transcriptomic profiling of mononuclear cells from IORT wound fluid samples reveals IL-6-JAK/STAT3-driven inflammatory activation

To explore whether immune cells recruited to the IORT site exhibit transcriptional alterations associated with irradiation-induced activation and/or polarization, we performed bulk RNA-sequencing on wound fluid cells isolated via Biocoll density gradient centrifugation (Figure 4, **Figure S4**). While this approach enriches for mononuclear cells, eosinophils—which were also elevated post-IORT—are underrepresented due to their higher density and partial loss during the separation process.

Pre-ranked gene set enrichment analysis (fGSEA) focusing on immune-related MSigDB Hallmark gene sets[15] identified significant enrichment of the IL-6-JAK/STAT3 signaling pathway in IORT

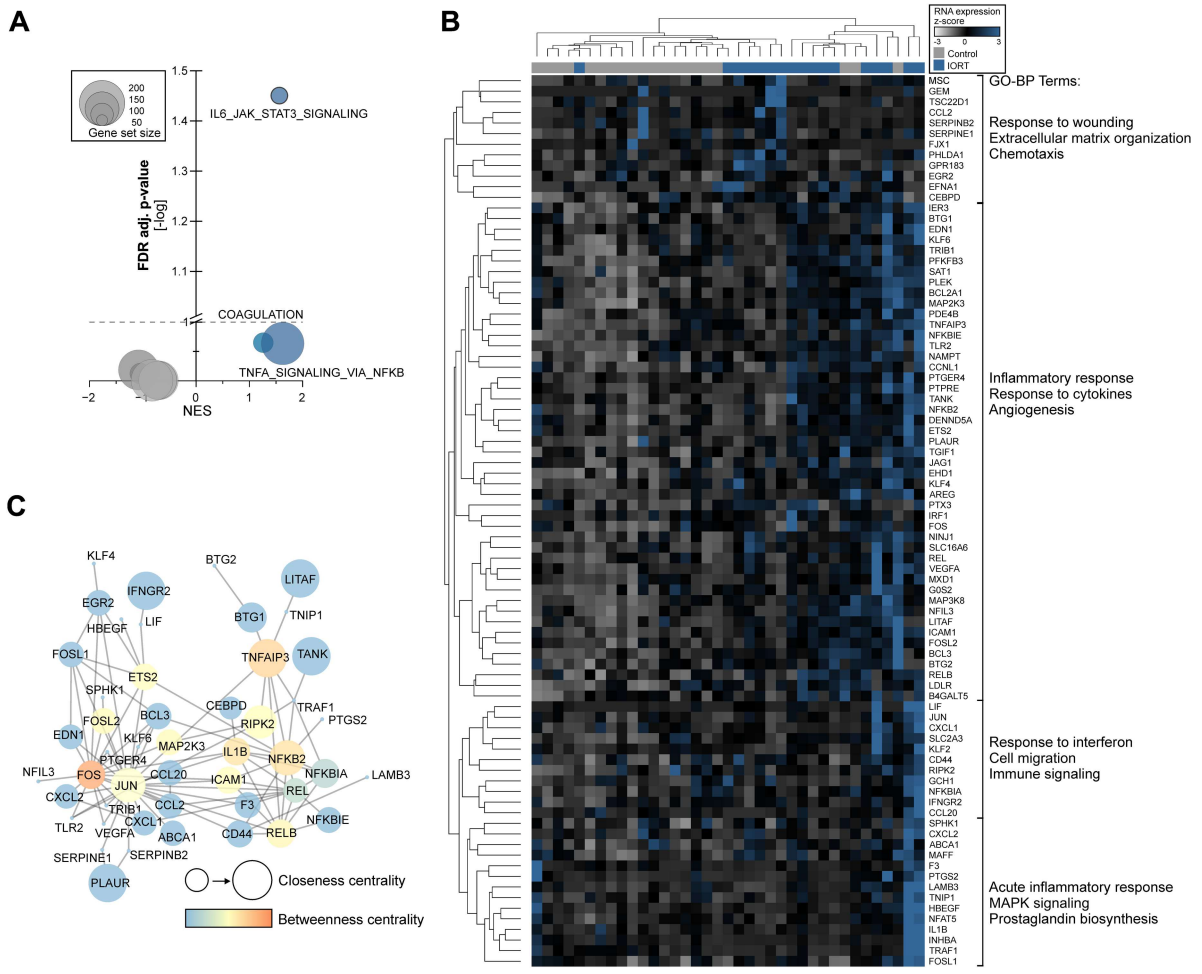

Figure 4. Transcriptomic profiling of mononuclear cells from IORT wound fluid samples reveals IL-6-JAK/STAT3-driven inflammatory activation. Mononuclear cells were isolated from day 2 wound fluid samples and subjected to 3′QuantSeq-based bulk RNA-sequencing. (A) Pre-ranked gene set enrichment analysis (fGSEA). IORT ($n = 17$) and control cases ($n = 20$) were compared using immune system-related MSigDB Hallmark gene sets. See also **Figure S4**. (B) Unsupervised hierarchical clustering of leading edge genes identified in (A) (Hallmark IL-6_JAK_STAT3_signaling gene set). Columns represent individual patients clustered by treatment group (IORT vs. control, Euclidean correlation distance). Gene clusters were annotated with Gene Ontology (GO-BP) terms. (C) Functional interaction network of leading edge genes identified in (A) (Hallmark IL-6_JAK_STAT3_signaling gene set), constructed with Cytoscape. Node size and color indicate closeness and betweenness centrality, respectively. Genes without connections are not shown.

samples compared to controls (Figure 4A). Unsupervised hierarchical clustering of leading edge genes within this gene set revealed distinct gene clusters, and Gene ontology (GO-BP) annotation provided further insights into their functional implications, including inflammatory signaling, cell migration, and innate immune cell activation (Figure 4B). Functional interaction network analysis of leading edge genes highlighted a densely interconnected module of inflammatory and transcriptional regulators (Figure 4C). Key transcription factors, such as FOS, JUN, REL, RELB, and NFKB2, emerged as central hubs, underscoring their pivotal roles in orchestrating the transcriptional response following IORT.

Overall, our findings delineate a scenario in which IORT triggers a localized and selective innate immune response—hallmarked by recruitment of pDCs, eosinophils, and monocytes into the irradiated tumor bed, and paralleled by their transient systemic mobilization. Cytokine profiling and *in vitro* modeling identify irradiated nonmalignant cells as key sources of recruitment factors, while transcriptomic analyses of wound fluid mononuclear cells reveal their increased activation as indicated by upregulated IL-6-JAK/STAT3 signaling.

Discussion

While the immunomodulatory potential of cancer radiotherapy is well documented in preclinical models, direct evidence from irradiated human tissues remains scarce and is largely limited to immune responses observed after radiotherapy in tumor-intact, neoadjuvant irradiation settings.[1,25,26] In clinical practice, however, radiotherapy is most commonly delivered in a postoperative, adjuvant setting, when minimal or no tumor burden remains within the radiation field. The immunological implications of radiotherapy in this postsurgical situation remain largely unexplored—preclinically due to lack of suitable model systems and trial designs, and clinically because access to irradiated tissue samples after surgery is extremely limited. In the present study, we made use of IORT during breast-conserving surgery to investigate early immune responses in irradiated postsurgical normal breast tissue *in situ*, in the absence of macroscopic tumor mass. This approach offers a rare, biologically informative, and clinically relevant opportunity to study both local and systemic immune dynamics following local irradiation in humans under real-world conditions.

Recently, a similar study examined human tissue responses following breast-conserving surgery ± IORT in the postsurgical setting.[27] These analyses focused on bulk RNA-sequencing data from re-excised margin tissue samples collected up to 15 d after surgery, thereby encompassing both early innate and later adaptive immune phases (11 IORT vs. 11 surgery-only cases). In contrast, our study investigates wound fluid derived directly from the postoperative tumor bed within the first three days after surgery, providing a focused assessment of the early innate immune response. Despite these methodological differences and the smaller sample size of the Orozco et al. report, gene expression profiles in both studies converge on signatures of inflammatory activation and immune cell recruitment. Importantly, our approach extends these findings by directly quantifying immune cell subsets and soluble mediators through multicolor flow cytometry and multiplex cytokine analyses, offering complementary cellular and protein-level resolution beyond transcriptomic enrichment analyses alone.

A striking observation in our study was the rapid and robust recruitment/retention of distinct innate immune cell subsets, particularly pDCs, eosinophils, and monocytes, in(to) the irradiated former tumor bed. These changes occurred within 2 d after IORT, indicating that localized high-dose radiation can act as a potent and rapid trigger of innate immune cell trafficking even in the absence of the bulk tumor mass and its potentially immunogenic cargo. Notably, two of these cell populations—monocytes and eosinophils—also revealed a transient increase in peripheral blood, peaking on day 3 after IORT. This systemic response likely reflects early mobilization of cells from hematopoietic reservoirs and may even involve emergency hematopoiesis, potentially triggered by cytokine gradients originating from the irradiated site. Importantly, preclinical models (of different entities including breast cancer) have not only demonstrated monocyte and eosinophil recruitment following irradiation of intact tumors in neoadjuvant-like settings, but also identified these cell types as critical mediators of radiotherapy efficacy, highlighting their essential roles in the (re-)activation of anti-tumor immune responses.[28,29] Our findings extend these insights to the clinical context in humans, and future follow-up analyses will clarify whether this has implications for local and/or systemic tumor control upon radiotherapy as has been reported for immune checkpoint blockade.[30-33]

Mechanistically, our data highlight MIF and IL-3 as potential orchestrators of early innate immune cell recruitment to irradiated sites. These cytokines were prominently elevated in wound fluid samples following IORT and correlated with the presence of specific innate immune subsets. MIF and IL-3 have well-characterized roles in normal tissue repair and early inflammation. MIF functions as a proinflammatory mediator released upon tissue injury and has been implicated in recruitment and activation of monocytes and other myeloid cells in sterile inflammatory contexts.[23,34-36] Likewise, IL-3 supports proliferation and differentiation of myeloid progenitors and can enhance the survival and function of granulocytic and monocytic lineages during early wound responses.[22,37-39] However, in tumor cell-containing environments, these same factors have also been implicated in protumorigenic processes. Elevated MIF expression by cancer cells or tumor-associated stroma can promote immunosuppressive myeloid phenotypes, enhance angiogenesis, and facilitate metastatic dissemination.[40-42] Similarly, increased IL-3 production has been linked to accelerated tumor progression and impaired prognosis.[43] These observations raise the theoretical

concern that IORT-induced elevation of MIF and IL-3 could, under certain conditions, counteract antitumor immunity—particularly in settings where residual tumor cells remain in the irradiated field (i.e. non-R0 surgical margins) and chronic signaling may sustain suppressive networks. Clinically, randomized trials of IORT in early breast cancer (e.g. TARGIT-A) have demonstrated overall comparable local control and survival outcomes between IORT plus risk-adapted external beam radiotherapy and non-IORT external beam radiotherapy, without evidence of increased relapse attributable to IORT-associated cytokine changes.[8] However, subgroup analyses directly comparing outcomes within R0 or non-R0 cases are not yet available. In the context of standard adjuvant external beam radiotherapy, which relies on lower fraction doses delivered over larger volumes of normal tissue, it remains unclear to what extent MIF, IL-3, or other cytokines are induced in healthy breast tissue. Limiting irradiation to the tumor bed through partial-breast techniques may potentially reduce cytokine-mediated immunomodulatory effects and mitigate undesired protumorigenic signaling. Such dose-confining strategies are increasingly applied in modern radiotherapy and are supported by several recent clinical and technical studies.[44,45]

Intriguingly, irradiation of primary nonmalignant cells *in vitro* recapitulated the cytokine profile observed upon IORT and induced features of cellular senescence, pointing to the irradiated nonmalignant tissue as a source of a radiation-induced senescence-associated secretory phenotype (SASP). While neither MIF nor IL-3 are canonical SASP factors, their induction suggests a broader secretory response priming the irradiated niche for innate immune cells, with MIF in particular known as a key mediator of monocyte as well as eosinophil recruitment in different preclinical models of inflammation. However, we cannot exclude that these cytokines were—at least in part—released by recruited immune cells rather than irradiated normal breast tissue cells alone. Moreover, wound fluid sampling likely underrepresents the full cytokine landscape due to limited analyte stability and dilution effects in this biosample, which is inherently of challenging quality. Nevertheless, the unique cytokine profile that we identified in IORT wound fluid samples likely reflects the distinct tissue context of postsurgical, localized radiation treatment. Unlike preclinical models, where irradiation of intact tumor cells promotes immune cell recruitment and activation through necrotic, immunogenic, or otherwise danger-associated cell death modalities—characterized by the release of danger signals such as ATP, HMGB1, heat shock proteins, and S100 proteins[1,2,5-7,46]—IORT primarily affects nonmalignant tissue with minimal residual tumor burden. We observed radiation-induced senescence in normal tissue cells rather than cell death, suggesting a distinct, proinflammatory, senescence-associated mechanism of immune cell recruitment that appears largely independent of the few remaining malignant cells within the former tumor bed.

Radiation-induced senescence has context-dependent effects: While it can limit proliferation and promote immune clearance via acute SASP signaling, chronic senescence in tumor-bearing tissues has been linked to immunosuppression, recurrence, and metastasis.[47,48] Our study captures early post-IORT responses in the absence of macroscopic tumor mass, reflecting acute wound healing rather than chronic tumor-associated remodeling. The observed cytokine elevations and innate immune recruitment likely represent transient inflammatory signaling. Consistently, clinical IORT trials in early breast cancer have not shown increased recurrence following IORT. Nevertheless, clinical and biological heterogeneity, including resection margin status, residual microscopic disease, and tumor-intrinsic susceptibility to SASP-mediated signaling, could modulate the impact of radiation-induced senescence on therapeutic outcome, highlighting the potential value of future personalized approaches.

The causal link between normal tissue cell senescence, cytokine release, and subsequent inflammatory immune cell recruitment is well established in radiation-induced normal tissue toxicities, such as pneumonitis, mucositis, and salivary gland atrophy.[49,50] While these adverse inflammatory effects of radiation are well documented, potentially beneficial, immune-modulatory effects upon focal high-dose irradiation of nonmalignant tissue remain understudied though such effects have been hypothesized.[51] Since the risk and severity of radiation-induced toxicities are closely linked to the volume of exposed tissue, the confined, high-dose delivery characteristic of IORT may limit long-term damage, yet still promote localized innate immune cell recruitment and activation, as observed in this study. Whether this innate immune response elicited by postsurgical breast cancer radiotherapy can subsequently trigger

antigen-specific adaptive immunity remains an open question, particularly in view of the limited availability of tumor antigen after surgical resection. Nevertheless, very recent clinical observations have provided promising evidence pointing into this direction.[52]

Taken together, our findings provide fundamental insights into local and systemic immune alterations following postsurgical breast cancer radiotherapy in humans, revealing that local irradiation of normal tissue is sufficient to trigger rapid and selective immune cell recruitment, with implications for optimizing radiotherapy-immunotherapy combinations in the clinic.

Limitations of the study

This study is limited by its focus on the very early immune events within the first 2 d after IORT, when wound fluids are available for analysis. Consequently, it primarily captures the innate immune phase and does not address adaptive immune mechanisms that underlie antigen-specific and durable antitumor immunity and typically emerge later. While correlations between cytokine levels and immune cell populations in the wound fluid were observed, the cellular sources of these cytokines remain unclear. Our data do not allow to determine whether the cytokines are produced locally by resident tissue cells—potentially driving immune cell recruitment—or are introduced into the wound environment by recruited immune cells. Functional assays to characterize the roles of these immune cells, and their contributions in tumor control and normal tissue responses were beyond the scope of this study. Finally, given its observational design, the study provides correlative rather than causal insights, as perturbational analyses are not feasible in this clinical setting.

Disclosure of potential conflicts of interest

The authors report there are no competing interests to declare.

Acknowledgments

We thank Paul Rühle for his support in establishing the immunophenotyping procedure. Parts of this manuscript have been previously published in the doctoral theses of A.T. and N.B. at the Medical Faculty, LMU Munich. Our special thanks go to the patients and their families for their willingness to participate in this observational study, for their trust in our research, and for their generous contribution to advancing our understanding of the immune effects of radiotherapy.

Author contributions

CRediT: **Anna Tiefenthaller:** Data curation, Formal analysis, Investigation, Methodology, Writing – review & editing; **Nikko Brix:** Conceptualization, Data curation, Formal analysis, Investigation, Methodology, Writing – original draft, Writing – review & editing; **Roman Hennel:** Investigation, Writing – review & editing; **Montserrat Pazos:** Investigation, Resources, Writing – review & editing; **Bernd Kost:** Investigation, Resources, Writing – review & editing; **Vera von Bodungen:** Investigation, Resources, Writing – review & editing; **Brigitte Rack:** Conceptualization, Investigation, Resources, Writing – review & editing; **Rachel Wuerstlein:** Investigation, Resources, Writing – review & editing; **Benjamin Frey:** Methodology, Resources, Writing – review & editing; **Udo S. Gaipl:** Methodology, Resources, Writing – review & editing; **Julia Hess:** Investigation, Writing – review & editing; **Kristian Unger:** Data curation, Formal analysis, Writing – review & editing; **Benedek Dankó:** Data curation, Formal analysis, Writing – review & editing; **Martin Selmansberger:** Data curation, Formal analysis, Writing – review & editing; **Horst Zitzelsberger:** Conceptualization, Funding acquisition, Resources, Writing – review & editing; **Nadia Harbeck:** Investigation, Resources, Writing – review & editing; **Claus Belka:** Conceptualization, Resources, Writing – review & editing; **Heike Scheithauer:** Conceptualization, Investigation, Resources, Writing – review & editing; **Kirsten Lauber:** Conceptualization, Data curation, Formal analysis, Funding acquisition, Investigation, Methodology, Project administration, Supervision, Visualization, Writing – original draft, Writing – review & editing.

Funding

This work was supported by the Bundesministerium fuer Forschung, Technologie und Raumfahrt BMFTR (DKTK, METABOLiST 02NUK061C, SeniRad 02NUK086A, and STRATUM 02NUK087), the Deutsche Forschungsgemeinschaft (DFG, INST 409/20-1 FUGG), the Heuer-Stiftung, and the Elite Netzwerk Bayern (iTarget Graduate Program).

ORCID

Nikko Brix 0009-0007-1266-1278
Kirsten Lauber 0000-0002-8141-0452

Data availability statement

RNA-sequencing data generated in this study have been deposited in the Gene Expression Omnibus (GEO) under accession number GSE302811. All other anonymized data supporting the findings of this study are available from the corresponding author upon reasonable request, subject to the constraints of the ethics approval and applicable GDPR regulations.

Ethics statement

The study was conducted between 2015 and 2025 (patient recruitment 2015–2018, biosample analyses 2015–2025) in accordance with the Declaration of Helsinki and was approved by the Ethics Committee of the LMU Munich Medical Faculty (approval numbers 246-15 and 20-488). Written informed consent was obtained from all participants prior to inclusion.

References

1. Guilbaud E, Naulin F, Meziani L, Deutsch E, Galluzzi L. Impact of radiation therapy on the immunological tumor microenvironment. Cell Chem Biol. 2025;32:678–693. doi: 10.1016/j.chembiol.2025.04.001.
2. Rodriguez-Ruiz ME, Vitale I, Harrington KJ, Melero I, Galluzzi L. Immunological impact of cell death signaling driven by radiation on the tumor microenvironment. Nat Immunol. 2020;21:120–134. doi: 10.1038/s41590-019-0561-4.
3. Lhuillier C, Rudqvist NP, Elemento O, Formenti SC, Demaria S. Radiation therapy and anti-tumor immunity: exposing immunogenic mutations to the immune system. Genome Med. 2019;11:40. doi: 10.1186/s13073-019-0653-7.
4. Brix N, Tiefenthaller A, Anders H, Belka C, Lauber K. Abscopal, immunological effects of radiotherapy: narrowing the gap between clinical and preclinical experiences. Immunol Rev. 2017;280:249–279. doi: 10.1111/imr.12573.
5. Wennerberg E, Vanpouille-Box C, Bornstein S, Yamazaki T, Demaria S, Galluzzi L. Immune recognition of irradiated cancer cells. Immunol Rev. 2017;280:220–230. doi: 10.1111/imr.12568.
6. Hennel R, Brix N, Seidl K, Ernst A, Scheithauer H, Belka C, Lauber K. Release of monocyte migration signals by breast cancer cell lines after ablative and fractionated gamma-irradiation. Radiat Oncol. 2014;9:85. doi: 10.1186/1748-717X-9-85.
7. Krombach J, Hennel R, Brix N, Orth M, Schoetz U, Ernst A, Schuster J, Zuchtriegel G, Reichel CA, Bierschenk S, et al. Priming anti-tumor immunity by radiotherapy: dying tumor cell-derived DAMPs trigger endothelial cell activation and recruitment of myeloid cells. Oncoimmunology. 2019;8:e1523097. doi: 10.1080/2162402X.2018.1523097.
8. Vaidya JS, Wenz F, Bulsara M, Tobias JS, Joseph DJ, Keshtgar M, Flyger HL, Massarut S, Alvarado M, Saunders C, et al. Risk-adapted targeted intraoperative radiotherapy versus whole-breast radiotherapy for breast cancer: 5-year results for local control and overall survival from the TARGIT-A randomised trial. Lancet. 2014;383:603–613. doi: 10.1016/S0140-6736(13)61950-9.
9. Vaidya JS, Bulsara M, Saunders C, Flyger H, Tobias JS, Corica T, Massarut S, Wenz F, Pigorsch S, Alvarado M, et al. Effect of delayed targeted intraoperative radiotherapy vs whole-breast radiotherapy on local recurrence and survival: long-term results from the TARGIT-A randomized clinical trial in early breast cancer. JAMA Oncol. 2020;6:e200249. doi: 10.1001/jamaoncol.2020.0249.
10. Sethi A, Emami B, Small W, Jr., Thomas TO. Intraoperative radiotherapy with INTRABEAM: technical and dosimetric considerations. Front Oncol. 2018;8:74. doi: 10.3389/fonc.2018.00074.
11. Schoetz U, Klein D, Hess J, Shnayien S, Spoerl S, Orth M, Mutlu S, Hennel R, Sieber A, Ganswindt U, et al. Early senescence and production of senescence-associated cytokines are major determinants of radioresistance in head-and-neck squamous cell carcinoma. Cell Death Dis. 2021;12:1162. doi: 10.1038/s41419-021-04454-5.
12. Danko B, Hess J, Unger K, Samaga D, Walz C, Walch A, Sun N, Baumeister P, Zeng PYF, Walter F, et al. Metabolic pathway-based subtypes associate glycan biosynthesis and treatment response in head and neck cancer. NPJ Precis Oncol. 2024;8:116. doi: 10.1038/s41698-024-00602-0.
13. Love MI, Huber W, Anders S. Moderated estimation of fold change and dispersion for RNA-seq data with DESeq2. Genome Biol. 2014;15:550. doi: 10.1186/s13059-014-0550-8.
14. Korotkevich G, Sukhov V, Budin N, Shpak B, Artyomov MN, Sergushichev A. Fast gene set enrichment analysis. bioRxiv, 2021:060012.
15. Liberzon A, Birger C, Thorvaldsdottir H, Ghandi M, Mesirov JP, Tamayo P. The molecular signatures database (MSigDB) hallmark gene set collection. Cell Syst. 2015;1:417–425. doi: 10.1016/j.cels.2015.12.004.

16. Shannon P, Markiel A, Ozier O, Baliga NS, Wang JT, Ramage D, Amin N, Schwikowski B, Ideker T. Cytoscape: a software environment for integrated models of biomolecular interaction networks. Genome Res. 2003;13:2498–2504. doi: 10.1101/gr.1239303.
17. Milacic M, Beavers D, Conley P, Gong C, Gillespie M, Griss J, Haw R, Jassal B, Matthews L, May B, et al. The reactome pathway knowledgebase 2024. Nucleic Acids Res. 2024;52:D672–D678. doi: 10.1093/nar/gkad1025.
18. Wuhrer A, Uhlig S, Tuschy B, Berlit S, Sperk E, Bieback K, Sutterlin M. Wound fluid from breast cancer patients undergoing intraoperative radiotherapy exhibits an altered cytokine profile and impairs mesenchymal stromal cell function. Cancers (Basel). 2021;13:2140. doi: 10.3390/cancers13092140.
19. Zindel J, Kubes P. DAMPs, PAMPs, and LAMPs in immunity and sterile inflammation. Annu Rev Pathol. 2020;15:493–518. doi: 10.1146/annurev-pathmechdis-012419-032847.
20. Liew PX, Kubes P. The Neutrophil's role during health and disease. Physiol Rev. 2019;99:1223–1248. doi: 10.1152/physrev.00012.2018.
21. Aliazis K, Yenyuwadee S, Phikulsod P, Boussiotis VA. Emergency myelopoiesis in solid cancers. Br J Haematol. 2024;205:798–811. doi: 10.1111/bjh.19656.
22. Weber GF, Chousterman BG, He S, Fenn AM, Nairz M, Anzai A, Brenner T, Uhle F, Iwamoto Y, Robbins CS, et al. Interleukin-3 amplifies acute inflammation and is a potential therapeutic target in sepsis. Sci. 2015;347:1260–1265. doi: 10.1126/science.aaa4268.
23. Bernhagen J, Krohn R, Lue H, Gregory JL, Zernecke A, Koenen RR, Dewor M, Georgiev I, Schober A, Leng L, et al. MIF is a noncognate ligand of CXC chemokine receptors in inflammatory and atherogenic cell recruitment. Nat Med. 2007;13:587–596. doi: 10.1038/nm1567.
24. Sumaiya K, Langford D, Natarajaseenivasan K, Shanmughapriya S. Macrophage migration inhibitory factor (MIF): a multifaceted cytokine regulated by genetic and physiological strategies. Pharmacol Ther. 2022;233:108024. doi: 10.1016/j.pharmthera.2021.108024.
25. Yoneyama M, Zormpas-Petridis K, Robinson R, Sobhani F, Provenzano E, Steel H, Lightowlers S, Towns C, Castillo SP, Anbalagan S, et al. Longitudinal assessment of tumor-infiltrating lymphocytes in primary breast cancer following neoadjuvant radiation therapy. Int J Radiat Oncol Biol Phys. 2024;120:862–874. doi: 10.1016/j.ijrobp.2024.04.065.
26. Shaitelman SF, Le-Petross H, Raso MG, Swanson DM, Schalck AP, Contreras A, Yang F, Muruganandham M, Zhao GZ, Sawakuchi GO, et al. PRECISE: preoperative radiation therapy to elicit critical immune stimulating Effects-A phase 2 clinical trial. Int J Radiat Oncol Biol Phys. 2025;121:90–96. doi: 10.1016/j.ijrobp.2024.08.008.
27. Orozco JIJ, Valdez BJ, Matsuba C, Simanonok MP, Ensenyat-Mendez M, Ramiscal JAB, Salomon MP, Takasumi Y, Grumley JG. Biological effects of intraoperative radiation therapy: histopathological changes and immunomodulation in breast cancer patients. Front Immunol. 2024;15:1373497. doi: 10.3389/fimmu.2024.1373497.
28. Tadepalli S, Clements DR, Saravanan S, Arroyo Hornero R, Ludtke A, Blackmore B, Paulo JA, Gottfried-Blackmore A, Seong D, Park S, et al. Rapid recruitment and IFN-I-mediated activation of monocytes dictate focal radiotherapy efficacy. Sci Immunol. 2023;8:eadd7446. doi: 10.1126/sciimmunol.add7446.
29. Cheng JN, Luo W, Sun C, Jin Z, Zeng X, Alexander PB, Gong Z, Xia X, Ding X, Xu S, et al. Radiation-induced eosinophils improve cytotoxic T lymphocyte recruitment and response to immunotherapy. Sci Adv. 2021;7. doi: 10.1126/sciadv.abc7609.
30. Krieg C, Nowicka M, Guglietta S, Schindler S, Hartmann FJ, Weber LM, Dummer R, Robinson MD, Levesque MP, Becher B. High-dimensional single-cell analysis predicts response to anti-PD-1 immunotherapy. Nat Med. 2018;24:144–153. doi: 10.1038/nm.4466.
31. Grisaru-Tal S, Itan M, Klion AD, Munitz A. A new Dawn for eosinophils in the tumour microenvironment. Nat Rev Cancer. 2020;20:594–607. doi: 10.1038/s41568-020-0283-9.
32. Voorwerk L, Garner H, Blomberg OS, Spagnuolo L, Chalabi E, MvD, Isaeva OI, Bakker N, Klaver C, Duijst M, Kersten K, et al. Critical role of eosinophils during response to immune checkpoint blockade in breast cancer and other cancer types. Ann Oncol. 2020;31:S1142. doi: 10.1016/j.annonc.2020.08.2237.
33. Zhou JG, Donaubauer AJ, Frey B, Becker I, Rutzner S, Eckstein M, Sun R, Ma H, Schubert P, Schweizer C, et al. Prospective development and validation of a liquid immune profile-based signature (LIPS) to predict response of patients with recurrent/metastatic cancer to immune checkpoint inhibitors. J Immunother Cancer. 2021;9:e001845. doi: 10.1136/jitc-2020-001845.
34. Stark K, Eckart A, Haidari S, Tirniceriu A, Lorenz M, von Bruhl ML, Gartner F, Khandoga AG, Legate KR, Pless R, et al. Capillary and arteriolar pericytes attract innate leukocytes exiting through venules and 'instruct' them with pattern-recognition and motility programs. Nat Immunol. 2013;14:41–51. doi: 10.1038/ni.2477.
35. Yoshihisa Y, Makino T, Matsunaga K, Honda A, Norisugi O, Abe R, Shimizu H, Shimizu T. Macrophage migration inhibitory factor is essential for eosinophil recruitment in allergen-induced skin inflammation. J Invest Dermatol. 2011;131:925–931. doi: 10.1038/jid.2010.418.
36. Magalhaes ES, Paiva CN, Souza HS, Pyrrho AS, Mourao-Sa D, Figueiredo RT, Vieira-de-Abreu A, Dutra HS, Silveira MS, Gaspar-Elsas MI, et al. Macrophage migration inhibitory factor is critical to interleukin-5-driven eosinophilopoiesis and tissue eosinophilia triggered by schistosoma mansoni infection. FASEB J. 2009;23:1262–1271. doi: 10.1096/fj.08-124248.

37. Warringa RA, Koenderman L, Kok PT, Kreukniet J, Bruijnzeel PL. Modulation and induction of eosinophil chemotaxis by granulocyte-macrophage colony-stimulating factor and interleukin-3. Blood. 1991;77:2694–2700. doi: 10.1182/blood.V77.12.2694.2694.
38. Li J, Zheng M, Ouyang F, Ye J, Huang J, Zhao Y, Wang J, Shan F, Li Z, Yu S, et al. Interleukin-3 modulates macrophage phagocytic activity and promotes spinal cord injury repair. CNS Neurosci Ther. 2024;30:e70181. doi: 10.1111/cns.70181.
39. Buelens C, Bartholome EJ, Amraoui Z, Boutriaux M, Salmon I, Thielemans K, Willems F, Goldman M. Interleukin-3 and interferon beta cooperate to induce differentiation of monocytes into dendritic cells with potent helper T-cell stimulatory properties. Blood. 2002;99:993–998. doi: 10.1182/blood.V99.3.993.
40. Zhang Z, Zhou X, Guo J, Zhang F, Qian Y, Wang G, Duan M, Wang Y, Zhao H, Yang Z, et al. TA-MSCs, TA-MSCs-EVs, MIF: their crosstalk in immunosuppressive tumor microenvironment. J Transl Med. 2022;20:320. doi: 10.1186/s12967-022-03528-y.
41. Youness RA, Elemam NM, Abdelhamid AM, Mohamed AH, Elsherbiny LM, Ramzy A, Assal RA. Macrophage migration inhibitory factor (MIF) and the tumor ecosystem: a tale of inflammation, immune escape, and tumor growth. Front Immunol. 2025;16:1636839. doi: 10.3389/fimmu.2025.1636839.
42. Noe JT, Mitchell RA. MIF-Dependent control of tumor immunity. Front Immunol. 2020;11:609948. doi: 10.3389/fimmu.2020.609948.
43. Thompson EJ, Escarbe S, Tvorogov D, Farshid G, Gregory PA, Khew-Goodall Y, Madden S, Ingman WV, Lindeman GJ, Lim E, et al. Interleukin-3 production by basal-like breast cancer cells is associated with poor prognosis. Growth Factors. 2024;42:49–61. doi: 10.1080/08977194.2023.2297693.
44. Vicini FA, Cecchini RS, White JR, Arthur DW, Julian TB, Rabinovitch RA, Kuske RR, Ganz PA, Parda DS, Scheier MF, et al. Long-term primary results of accelerated partial breast irradiation after breast-conserving surgery for early-stage breast cancer: a randomised, phase 3, equivalence trial. Lancet. 2019;394:2155–2164. doi: 10.1016/S0140-6736(19)32514-0.
45. Viani GA, Arruda CV, Faustino AC, De Fendi LI. Partial-breast irradiation versus whole-breast radiotherapy for early breast cancer: a systematic review and update meta-analysis. Brachytherapy. 2020;19:491–498. doi: 10.1016/j.brachy.2020.03.003.
46. Demaria S, Formenti SC. Role of T lymphocytes in tumor response to radiotherapy. Front Oncol. 2012;2:95. doi: 10.3389/fonc.2012.00095.
47. Faget DV, Ren Q, Stewart SA. Unmasking senescence: context-dependent effects of SASP in cancer. Nat Rev Cancer. 2019;19:439–453. doi: 10.1038/s41568-019-0156-2.
48. McHugh D, Duran I, Gil J. Senescence as a therapeutic target in cancer and age-related diseases. Nat Rev Drug Discov. 2025;24:57–71. doi: 10.1038/s41573-024-01074-4.
49. Cytlak UM, Dyer DP, Honeychurch J, Williams KJ, Travis MA, Illidge TM. Immunomodulation by radiotherapy in tumour control and normal tissue toxicity. Nat Rev Immunol. 2022;22:124–138. doi: 10.1038/s41577-021-00568-1.
50. De Ruysscher D, Niedermann G, Burnet NG, Siva S, Lee AWM, Hegi-Johnson F. Radiotherapy toxicity. Nat Rev Dis Primers. 2019;5:13. doi: 10.1038/s41572-019-0064-5.
51. Vaidya JS, Bulsara M, Baum M, Wenz F, Massarut S, Pigorsch S, Alvarado M, Douek M, Saunders C, Flyger H, et al. New clinical and biological insights from the international TARGIT-A randomised trial of targeted intraoperative radiotherapy during lumpectomy for breast cancer. Br J Cancer. 2021;125:380–389. doi: 10.1038/s41416-021-01440-8.
52. Dai D, Li X, Zhuang H, Ling Y, Chen L, Long C, Zhang J, Wang Y, Li Y, Tang H, et al. Landscape of the peripheral immune response induced by intraoperative radiotherapy combined with surgery in early breast cancer patients. Adv Sci (Weinh). 2025;12:e2308174. doi: 10.1002/advs.202308174.